

# Preparation of barium titanate hollow particle by two-step chemical solution deposition

Tomoya OHNO,<sup>†</sup> Tomoyuki SUGIURA, Shinji WATANABE, Hisao SUZUKI\* and Takeshi MATSUDA

Department of Materials Science, Kitami Institute of Technology, 165 Koen-cho, Kitami, Hokkaido 090–8507, Japan

\*Graduate School of Science and Technology, Shizuoka University, 3–5–1 Johoku, Hamamatsu 432–8561, Japan

Barium titanate (BTO) hollow particles were prepared using two-step chemical solution deposition with a template particle. Polystyrene (PSt) was selected as the template particle, and N-(hydroxymethyl)acrylamide (HMAm) was polymerized as a comonomer to generate the hydrophilic group on the PSt template particle surface. The BTO monophase was attained at  $[Ba]/[TiO_2] = 1.0$  using 350°C pre-annealed  $TiO_2$  precursor hollow particles. The obtained BTO particle was a hollow structure with shell thickness of approximately 45 nm. The surface area of the obtained BTO hollow particle was 12 m<sup>2</sup>/g, which was approximately twice as large as that of alkoxide-derived BTO particles created with the same annealing temperature.

©2013 The Ceramic Society of Japan. All rights reserved.

Key-words : Perovskite material, High surface area, Catalyst, Chemical solution deposition, Nanocoating

[Received July 23, 2012; Accepted November 11, 2012]

## 1. Introduction

Barium titanate (BTO) is an important material for use in electric and optic devices because of its excellent properties.<sup>1),2)</sup> Lately, Ni on perovskite material (Ni/Perovskite) has received much attention as a catalyst for methane steam reforming and partial oxidation of  $CH_4$ .<sup>3),4)</sup> For example, Takehira et al. reported that perovskite-type oxides such as BTO exhibit high catalytic activities with high resistance to coking in partial oxidation of methane.<sup>3)</sup> However, in almost all cases, the perovskite material surface area has been reported as very small (less than 10 m<sup>2</sup>/g). In general, the catalytic activity depends strongly on the surface area. Perovskite materials with a large surface area are necessary for use as novel catalysts for steam reforming processes.

In our previous study, we prepared core-shell type BTO– $SiO_2$  hybrid nanoparticles with 20 m<sup>2</sup>/g using two-step chemical solution deposition. In addition, the obtained BTO– $SiO_2$  catalyst was applied to methane steam reforming.<sup>5)</sup> Results show that the methane conversion ratio of this material was approximately three times as large as that of the reported BTO catalyst,<sup>4)</sup> even at a lower processing temperature. However, the temperature limit of this material was 600°C because of the generation of  $Ba_2(TiO)Si_2O_7$  phase during steam reforming, which is attributable to the diffusion of Ba component to  $SiO_2$  core particles during the process. This study was conducted to prepare BTO hollow particles to resolve this subject.

The strategy for fabricating inorganic hollow particles is of intense interest because of its potential applications for drug delivery,<sup>6)</sup> optic devices,<sup>7)</sup> photocatalysts,<sup>8)</sup> and catalysts.<sup>9)</sup> Many researchers have reported chemical and physicochemical methods such as heterophase polymerizations combined with the sol-gel process,<sup>10)</sup> emulsion polymerization strategies,<sup>11)</sup> and nozzle reactor approaches<sup>12)</sup> to prepare hollow structures of various materials. However, fabrication of the hollow particle with complex oxides (such as BTO) still presents some subjects, such

as difficulties of the control of chemical reaction and precipitation. For two-step chemical solution deposition, each component is nanocoated separately onto the template core-particles, and a complex oxide is obtained using thermal diffusion process. Therefore, this process is effective to attain the nanocoating of complex oxides on the core-particles.<sup>5)</sup> For this study, we attempted to prepare BTO hollow particles in a two-step chemical solution deposition using template core particles.

## 2. Experimental procedure

Polystyrene (PSt) core particles were prepared by emulsion polymerization as template core particles. For this study, N-(hydroxymethyl)acrylamide (HMAm) was also polymerized as a comonomer to generate the hydrophilic group on the PSt template particle surface ( $[HMAm]:[St] = 1:19$ ). Additionally, hexanol was impregnated into the obtained PSt-HMAm template particles to increase the hydrophilic group on the surface. The experimental details are described elsewhere.<sup>13)</sup> As the first step of chemical solution deposition,  $TiO_2$  layer was nanocoated onto the surface of PSt-HMAm core particles using liquid phase deposition. The starting reagents were ammonium hexafluorotitanate (IV), boric acid, and the obtained PSt-HMAm sol. The boric acid concentration was adjusted to 0.7 M. The molar ratio of  $[boric\ acid]:[Ti]$  was adjusted to 5.0. The experimental details are described elsewhere.<sup>14),15)</sup> Subsequently, the obtained  $TiO_2$ -PSt hybrid particles were pre-annealed at 350°C or 600°C for 1 h to remove the template particle. As the second step of the two-step chemical solution deposition, the Ba component was loading to  $TiO_2$  hollow particles using a Ba alkoxide precursor solution. The starting reagent of Ba precursor solution was metal Ba. The metal Ba was dissolved in ethanol with 0.1 M concentration. The Ba-doped  $TiO_2$  hollow particles were pre-annealed at 350°C. Then final annealing was conducted at 800°C to produce BTO hollow particles. After final annealing, the obtained hollow particles were washed using distilled water and HCl to remove the fluoride and barium carbonate.

To compare the surface area of the obtained BTO particles, alkoxide-derived BTO particles were also prepared using chemi-

<sup>†</sup> Corresponding author: T. Ohno; E-mail: ohno@mail.kitami-it.ac.jp

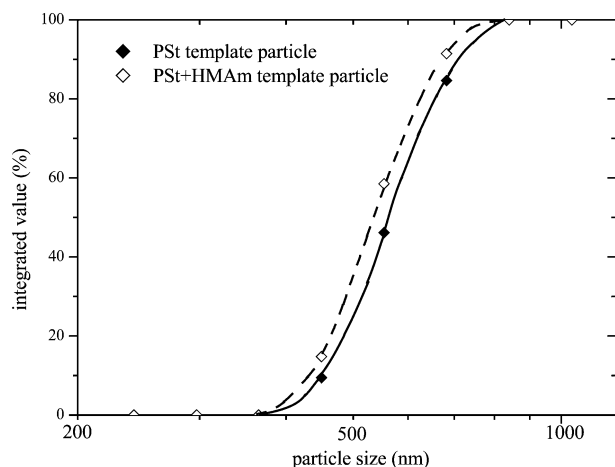


Fig. 1. Particle distributions of PSt and PSt+HMAM template particles.

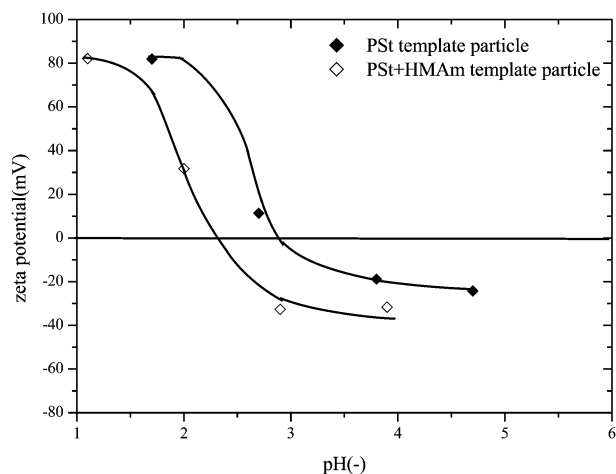
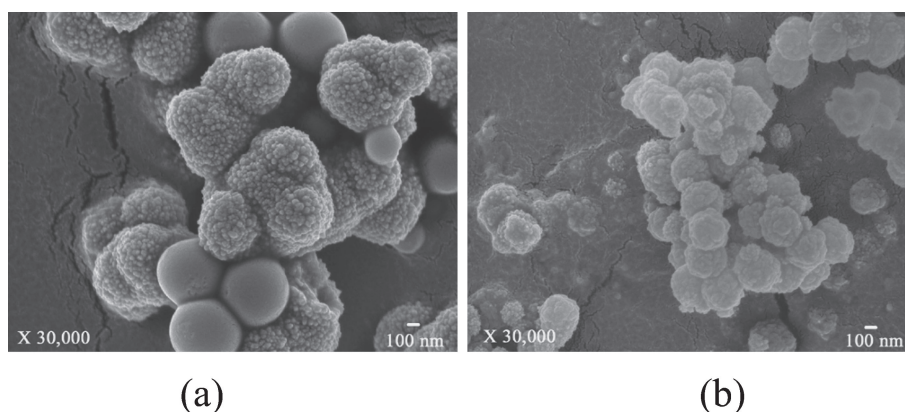


Fig. 2. Change in the zeta potential of core particles as a function of pH.

Fig. 3. SEM images of the obtained  $\text{TiO}_2$  nanocoated template particles: (a)  $\text{TiO}_2$ -PSt hybrid particle, and (b)  $\text{TiO}_2$ -PSt+HMAM hybrid particle.

cal solution deposition. The starting reagents of BTO precursor solution are metal barium and titanium iso-propoxide. The metal Ba and the titanium iso-propoxide were dissolved separately in ethanol at room temperature. Subsequently the obtained titanium and barium precursor solutions were mixed at room temperature for 1 h to obtain the BTO precursor solution. The BTO precursor particle was prepared by evaporating the solvent from the BTO precursor solution. The as-deposited BTO precursor particles were pre-annealed and annealed respectively at 350 and 800°C.

The crystal structure of the obtained BTO hollow particles was measured using X-ray diffraction (XRD, D4 Endeavor; Bruker AXS GmbH). The morphology of the obtained particles was confirmed using transmission electron microscopy (TEM, H-9000 NAR; Hitachi Ltd.) and scanning electron microscopy (FE-SEM; with Carl Zeiss Supra 35 VP, JSM 5800; JEOL). Then the specific surface area was estimated by the absorption isotherm of  $\text{N}_2$  using the BET (Brunauer–Emmett–Teller) equation. The sample was evaluated 300°C for 0.5 h. The adsorption isotherm  $\text{N}_2$  was measured at  $-196^\circ\text{C}$  using a conventional high-vacuum static system.

### 3. Results

#### 3.1 Template particle diameter

Watanabe et al. reported that the HMAM is an effective comonomer not only for the generation of hydrophilic groups on the surface but also for decreasing the particle size.<sup>13)</sup> Therefore,

effects of the HMAM on the particle diameter were estimated as determined by the template particle size. **Figure 1** presents the size distribution of the PSt and PSt+HMAM template particles. Results show that the respective 50% volume particle sizes of PSt and PSt+HMAM particles were approximately 560 and 530 nm. In addition, the size distribution ( $\Delta d/d$ ) was approximately 0.3 in both cases. In general, the small template particle has large surface area in the case of hollow particles. Therefore, we selected the PSt+HMAM particles for use as template particles in this study.

#### 3.2 Effects of the surface treatment of template particles on the $\text{TiO}_2$ nanocoating

For liquid-phase deposition, a hydrophilic group on the core particles is necessary for the homogeneous nanocoating process.<sup>14),15)</sup> Therefore, the surface treatment of template particle was attempted using comonomer (HMAM) to attain the homogeneous  $\text{TiO}_2$  nanocoating on the template. **Figure 2** presents a change in the zeta potential of template particles as a function of pH. The iso-electric point (IEP) of PSt with HMAM was approximately 2.3, although that of PSt was 2.9. This result indicates that the hydrophilic group was increased by surface treatment. **Figure 3** portrays SEM images of the obtained  $\text{TiO}_2$  nanocoated template particles. For PSt with HMAM template particle, a homogeneous  $\text{TiO}_2$  nanocoating was obtained, but an inhomogeneous  $\text{TiO}_2$  nanocoating was confirmed in the case of PSt template particles.

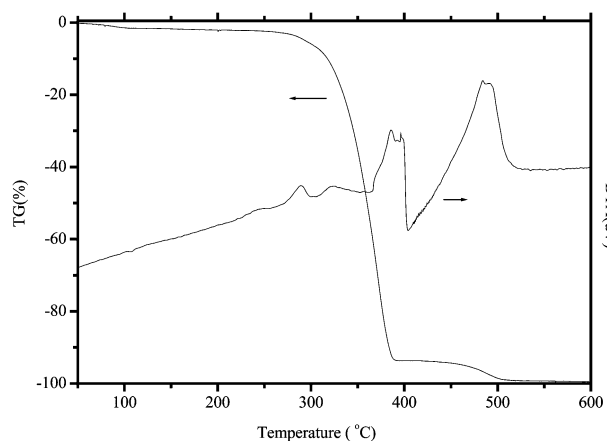


Fig. 4. Thermal analysis of PSt+HMAm particle.

In addition, the  $\text{TiO}_2$ -PSt particle diameter was larger than that of the  $\text{TiO}_2$ -PSt+HMAm because of the different particle size of template particles. This result illustrates the surface treatment as effective to generate the hydrophilic group on the template particles, producing homogeneous  $\text{TiO}_2$  nanocoating by liquid phase deposition.

### 3.3 Removing the template particle

TG-DTA analysis was conducted to determine the pre-annealing temperature for removal of the PS+HMAm template particle. **Figure 4** shows the TG-DTA analysis of the PSt+HMAm template particle. PSt and HMAm were thermally decomposed, respectively, at 350 and 500°C. The HMAm component, which was added as copolymerization, mostly remained at 350°C. Pre-annealing was conducted at 350°C because a smaller  $\text{TiO}_2$  crystal size is effective to prepare BTO with perovskite monophase by lower annealing temperature. In contrast, pre-annealing was also conducted at 600°C to elucidate the effect of the residual HMAm and  $\text{TiO}_2$  crystal size on the BTO crystal phase.

### 3.4 Effect of $[\text{Ba}]/[\text{TiO}_2]$ ratio on the crystal phase

For liquid phase deposition, the determination of the yield of the coating material is difficult. Therefore, we assumed that the obtained  $\text{TiO}_2$  hollow particles were pure titania without impurity. Under the above consideration,  $[\text{Ba}]/[\text{TiO}_2]$  ratio was changed in the range of 0.6 to 1.0 for determination of the appropriate amount of Ba component to prepare pure BTO. **Figure 5** depicts the XRD patterns of the obtained BTO with different  $[\text{Ba}]/[\text{TiO}_2]$  ratio. For 600°C pre-annealed  $\text{TiO}_2$  precursor particle, all resultant BTO particles include  $\text{Ba}_2\text{TiO}_4$ ,  $\text{BaCO}_3$ , and  $\text{TiO}_2$  phase. This result shows that the thermal diffusion of the Ba component was insufficient even in 800°C annealing because the crystal size of  $\text{TiO}_2$  was large. In contrast, in the case of 350°C pre-annealed  $\text{TiO}_2$  precursor particle,  $\text{Ba}_2\text{TiO}_4$  and  $\text{TiO}_2$  phase can not confirm which could be attributable to the crystallite size of  $\text{TiO}_2$  hollow particles, although a faint amount of HMAm remains in the precursors. However,  $\text{BaF}_2$  phase existed, which can be attributable to the reaction between the residual F during  $\text{TiO}_2$  nanocoating process and Ba component. Subsequently, the obtained samples were washed using distilled water and HCl to remove the  $\text{BaF}_2$  and a trace amount of  $\text{BaCO}_3$ . **Figure 6** shows the effects of washing on the crystal phase of the obtained BTO hollow particles. After washing with distilled water,  $\text{BaF}_2$  phase was removed clearly, and the  $\text{BaCO}_3$  phase was removed by HCl washing. Finally, the

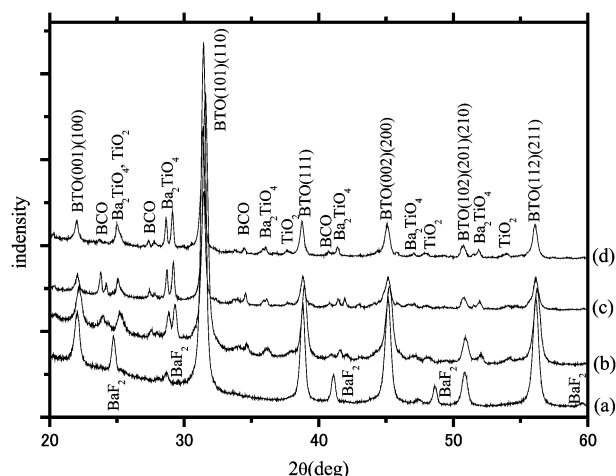


Fig. 5. XRD patterns of the obtained BTO hollow particles with different  $[\text{Ba}]/[\text{TiO}_2]$  ratios: (a)  $[\text{Ba}]/[\text{TiO}_2] = 1.0$  350°C pre-annealing, (b)  $[\text{Ba}]/[\text{TiO}_2] = 1.0$ , (c)  $[\text{Ba}]/[\text{TiO}_2] = 0.8$ , and (d)  $[\text{Ba}]/[\text{TiO}_2] = 0.6$ . Pre-annealing of (b), (c), (d) was conducted at 600°C.

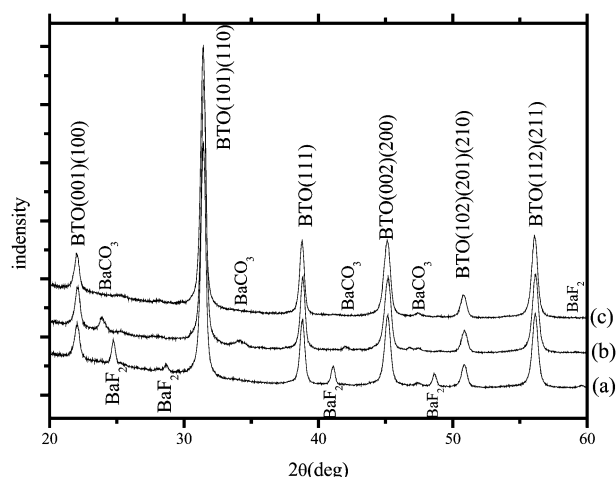


Fig. 6. XRD patterns of the obtained BTO hollow particles after washing: (a) as-deposited, (b) after washing with distilled water, and (c) after washing with distilled water and HCl.

perovskite mono-phase with hollow structure was obtained using two-step chemical solution deposition.

### 3.5 Microstructure of the obtained BTO hollow particles

**Figure 7** displays TEM images of the resultant BTO hollow particles. From TEM images, the microstructure of the obtained particle was inferred as a hollow structure. The BTO hollow particle size was approximately 200 nm, although the template particle size was approximately 480 nm. This reason derived from shrinkage of the obtained hollow particles during the removal process of template and the annealing processing. The BTO crystal size was calculated as 22 nm using Scherrer's equation. In addition, the average shell thickness was approximately 45 nm. Therefore, it was concluded that the BTO shell consists of double layers of BTO nanocrystals. The surface area of the obtained BTO hollow particles was approximately 12  $\text{m}^2/\text{g}$ . Alkoxide-derived BTO particles were also prepared to ascertain the effect of particle structure on the surface area. **Figure 8** shows an SEM image and the particle distribution of

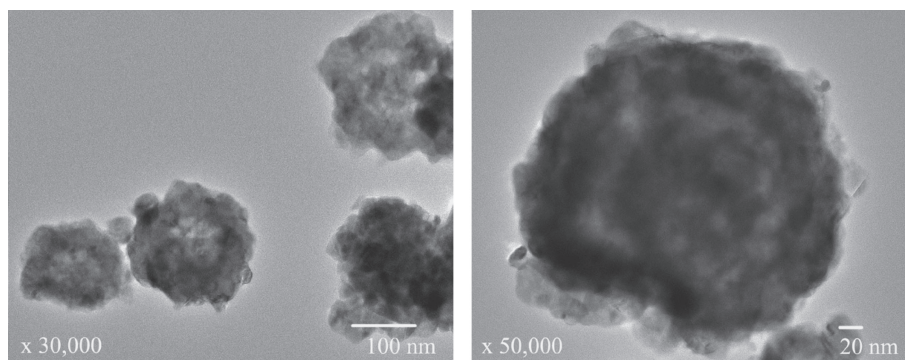


Fig. 7. TEM images of the obtained BTO hollow particles.

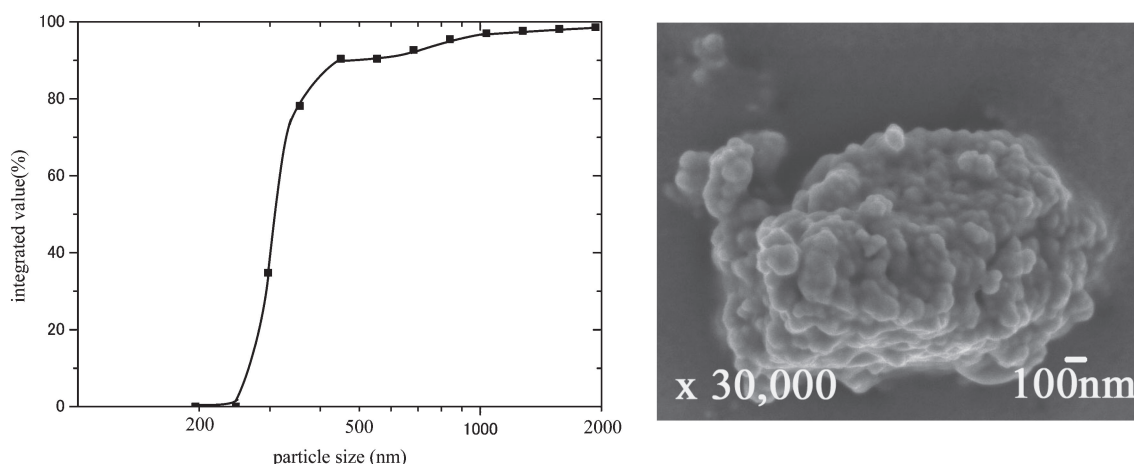


Fig. 8. Data of alkoxide-derived BTO particles with 800°C annealing temperature: (a) particle size distribution, and (b) SEM image.

the alkoxide-derived BTO particles, and shows a few secondarily coagulated particles observed at around 1  $\mu\text{m}$  particle diameter, although the primary particle diameter was nearly the same as that of the hollow particles. In addition, the crystallite size was almost the same (22 nm) because of its equivalent annealing temperature. However, in the case of alkoxide derived BTO powder, the surface area was approximately 5  $\text{m}^2/\text{g}$ . Therefore, we concluded that preparation of the hollow structure was effective for obtaining perovskite materials with large surface area because of the suppressed coagulation of nanocrystals.

#### 4. Conclusions

BTO hollow particles were prepared using chemical solution deposition in two steps with a template particle. The template particle of PSt+HMAM was prepared by emulsion polymerization. HMAM was an effective comonomer to apply the hydrophilic group on the surface of template particle, resulting in the homogeneous  $\text{TiO}_2$  nanocoating on the template particle. The Ba component was loaded to  $\text{TiO}_2$  hollow particles using a Ba alkoxide. In this study, BTO monophasic was attained at  $[\text{Ba}]/[\text{TiO}_2] = 1.0$  using 350°C pre-annealed  $\text{TiO}_2$  hollow particles. The BTO hollow particle surface area was 12  $\text{m}^2/\text{g}$ . This value was approximately twice as large as that of the alkoxide-derived BTO particles at the same annealing temperature. Therefore, we concluded that preparation of the hollow structure is an effective means to obtain perovskite materials having a large surface area.

#### References

- 1) C. E. Folgar, C. Suchicital and S. Priya, *Mater. Lett.*, **65**, 1302–1307 (2011).
- 2) G. Yang, Y. Zhou, H. Long, Y. Li and Y. Yang, *Thin Solid Films*, **515**, 7926–7929 (2007).
- 3) K. Takehira, T. Shishido and M. Kondo, *J. Catal.*, **207**, 307–316 (2002).
- 4) K. Urasaki, Y. Sekine, S. Kawabe, E. Kikuchi and M. Matsukawa, *Appl. Catal., A*, **286**, 23–29 (2005).
- 5) T. Ohno, K. Numakura, H. Suzuki and T. Matsuda, *Mater. Chem. Phys.*, **134**, 514–517 (2012).
- 6) H. Ai, *Adv. Drug Deliv. Rev.*, **63**, 772–788 (2011).
- 7) T. H. Kim, K. H. Lee and Y. K. Kwon, *J. Colloid Interface Sci.*, **304**, 370–377 (2006).
- 8) T. Tseng, J. Uan and W. J. Tseng, *Ceram. Int.*, **37**, 1775–1780 (2011).
- 9) X. Yang, S. Liao, J. Zeng and Z. Liang, *Appl. Surf. Sci.*, **257**, 4472–4477 (2011).
- 10) R. Muñoz-Espi, C. K. Weiss and K. Landfester, *Curr. Opin. Colloid Interface Sci.*, **17**, 212–224 (2012).
- 11) L. Zhang, P. Liu and T. Wang, *Chem. Eng. J.*, **171**, 711–716 (2011).
- 12) A. B. D. Nandiyanto and K. Okuyama, *Adv. Powder Technol.*, **22**, 1–19 (2011).
- 13) S. Watanabe, R. Ikeda, H. Kitagawa, M. Murata and Y. Masuda, *Macromol. Chem. Phys.*, **201**, 896–901 (2000).
- 14) T. Ohno, K. Numakura, H. Itoh, H. Suzuki and T. Matsuda, *Mater. Lett.*, **63**, 1737–1739 (2009).
- 15) T. Ohno, K. Numakura, H. Itoh, H. Suzuki and T. Matsuda, *Adv. Powder Technol.*, **22**, 390–395 (2011).